Metabolic Engineering Communications 14 (2022) e00196

Contents lists available at ScienceDirect

Metabolic Engineering Communications

journal homepage: www.elsevier.com/locate/mec

Development of an *E. coli*-based norbaeocystin production platform and evaluation of behavioral effects in rats

Alexandra M. Adams [a], Nicholas A. Anas [b], Abhishek K. Sen [a], Jordan D. Hinegardner-Hendricks [b], Philip J. O'Dell [a], William J. Gibbons Jr. [a], Jessica E. Flower [a], Matthew S. McMurray [b,*], J. Andrew Jones [a,**]

[a] *Miami University, Department of Chemical, Paper, and Biomedical Engineering, Oxford, OH, 45056, USA*
[b] *Miami University, Department of Psychology, Oxford, OH, 45056, USA*

ARTICLE INFO

Keywords:
Norbaeocystin
Psilocybin
Head twitch response
Psychedelic medicine
Depression
Long-Evans rat

ABSTRACT

Interest in the potential therapeutic efficacy of psilocybin and other psychedelic compounds has escalated significantly in recent years. To date, little is known regarding the biological activity of the psilocybin pathway intermediate, norbaeocystin, due to limitations around sourcing the phosphorylated tryptamine metabolite for *in vivo* testing. To address this limitation, we first developed a novel *E. coli* platform for the rapid and scalable production of gram-scale amounts of norbaeocystin. Through this process we compare the genetic and fermentation optimization strategies to that of a similarly constructed and previously reported psilocybin producing strain, uncovering the need for reoptimization and balancing upon even minor genetic modifications to the production host. We then perform *in vivo* measurements of head twitch response to both biosynthesized psilocybin and norbaeocystin using both a cell broth and water vehicle in Long-Evans rats. The data show a dose response to psilocybin while norbaeocystin does not elicit any pharmacological response, suggesting that norbaeocystin and its metabolites may not have a strong affinity for the serotonin 2A receptor. The findings presented here provide a mechanism to source norbaeocystin for future studies to evaluate its disease efficacy in animal models, both individually and in combination with psilocybin, and support the safety of cell broth as a drug delivery vehicle.

1. Introduction

Norbaeocystin (3-(2-aminoethyl)-1H-indol-4-yl dihydrogen phosphate) is a tryptamine intermediate product in the psilocybin biosynthesis pathway that has been hypothesized to have its own neurological activity due to its structural similarity to psilocybin (Leung and Paul, 1968; Sherwood et al., 2020). Psilocybin-containing mushroom users have also reported a range of experiences linked to the various strains of mushrooms, which contain varying amounts of psilocybin and its minor metabolites, especially norbaeocystin and baeocystin (Gartz, 1994; Wurst et al., 2002). However, limited peer-reviewed studies exist on this topic due to the legal restrictions surrounding psilocybin and difficulty sourcing specific minor metabolites for testing, until recently (Sherwood et al., 2020). The structural similarity suggests that psilocybin pathway intermediates may also have similar binding sites or metabolic processes to psilocybin. These anecdotal reports of varied, species-specific, hallucinogenic experiences by recreational mushroom users are motivation for this study to explore the specific pharmacological effects of norbaeocystin and psilocybin in a rat model.

An initial challenge to this study was that no natural sources are currently available that specifically over-produce norbaeocystin, a key precursor to psilocybin, and only recently has a synthetic route been published for its production (Sherwood et al., 2020). This current synthesis strategy is also resource-intensive, posing additional challenges to

* Corresponding author. Miami University, Department of Psychology Center for Neuroscience and Behavior 221 Psychology, Building 90 N Patterson Ave.
** Corresponding author. Miami University, Department of Chemical, Paper, and Biomedical Engineering, 64P Engineering Building 650 E. High St, Oxford, OH, 45056.
E-mail addresses: adamsam8@miamioh.edu (A.M. Adams), anasna@miamioh.edu (N.A. Anas), sena2@miamioh.edu (A.K. Sen), hinegajd@miamioh.edu (J.D. Hinegardner-Hendricks), odellpj@miamioh.edu (P.J. O'Dell), gibbonwj@miamioh.edu (W.J. Gibbons), flowerj4@miamioh.edu (J.E. Flower), mcmurrms@miamioh.edu (M.S. McMurray), jones@miamioh.edu (J.A. Jones).

https://doi.org/10.1016/j.mec.2022.e00196
Received 10 January 2022; Received in revised form 3 March 2022; Accepted 10 March 2022
Available online 12 March 2022
2214-0301/© 2022 The Authors. Published by Elsevier B.V. on behalf of International Metabolic Engineering Society. This is an open access article under the CC BY-NC-ND license (http://creativecommons.org/licenses/by-nc-nd/4.0/).

its use in behavioral research. As an alternative to synthetic production, psilocybin biosynthesis in a variety of recombinant host organisms has demonstrated recent success (Adams et al., 2019; Milne et al., 2020). Building off this work, we show that biosynthetic production of norbaeocystin by recombinant *Escherichia coli* is not only feasible but can surpass the key production metrics (titer, productivity, and yield) reported previously for psilocybin by our research group (Adams et al., 2019). Surprisingly, we found that the genetic optimization parameters ideal for psilocybin bioproduction did not translate to those found for norbaeocystin bioproduction. Upon optimization, the recombinant expression of two previously reported (Adams et al., 2019) enzymes from *Psilocybe cubensis,* an L-tryptophan decarboxylase (PsiD) and a kinase (PsiK), coupled with the promiscuity of *E. coli*'s native tryptophan synthase (TrpB) led to a norbaeocystin production platform (Fig. 1b) capable of producing 1.58 ± 0.08 g/L of norbaeocystin in a benchtop bioreactor. We then tested the effectiveness of psilocybin and norbaeocystin at eliciting Head Twitch Responses (HTRs), also referred to as Wet Dogs Shakes, in Long-Evans rats. These motions are high-frequency paroxysmal head and body rotations that occur in rodents after 5-HT2A receptor activation (Canal and Morgan, 2012; Halberstadt and Geyer, 2011, 2013). This behavior is widely used as an indicator of hallucinogenic effects and it is one of the only behaviors that can reliably distinguish hallucinogenic from non-hallucinogenic 5-HT2A agonists (de la Fuente Revenga et al., 2019; González-Maeso et al., 2007). We found that E. coli-derived psilocybin caused dose-dependent increases in HTRs, while norbaeocystin did not. Together, these studies motivate the

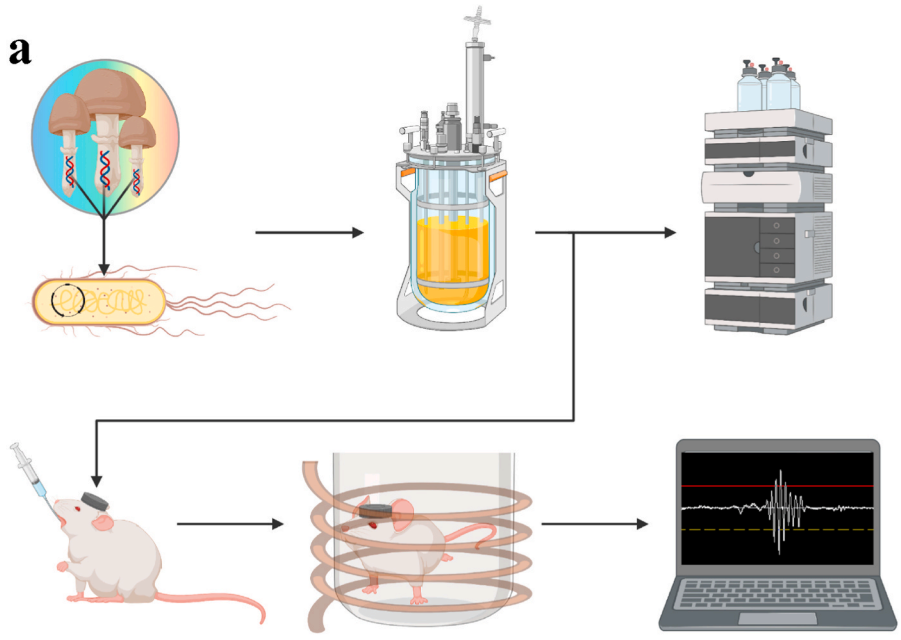

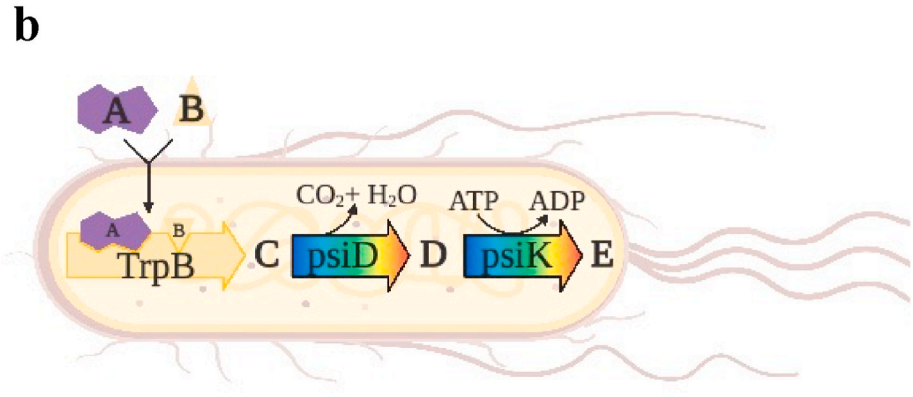

(A)	(B)	(C)	(D)	(E)
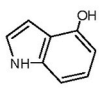	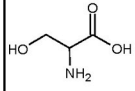	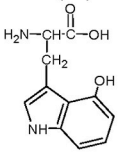	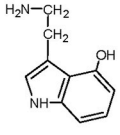	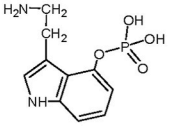
4-hydroxyindole	serine	4-hydroxytryptophan	4-hydroxytryptamine	norbaeocystin

Fig. 1. (a) Overview of study methods. Recombinant *E. coli* were developed capable of high-level norbaeocystin production. Norbaeocystin production was optimized and scaled up in a benchtop bioreactor. Norbaeocystin concentration in cell broth was quantified using HPLC. A rat with a magnet affixed to its head was gavaged with psilocybin or norbaeocystin in either a cell broth or water vehicle. A magnetometer coil was used in order to record head twitches. Waveforms were then analyzed to determine the head twitch count. (b) Norbaeocystin biosynthesis pathway. The *E. coli* strain contains three genes, one native (*trpB*) and two heterologous (*psiD*, *psiK*) that enable norbaeocystin biosynthesis from external supplementation of 4-hydroxyindole. Tryptophan synthase (TrpB) condenses 4-hydroxyindole and serine to form 4-hydroxytryptophan. *P. cubensis* tryptophan decarboxylase (PsiD) converts 4-hydroxytryptophan into 4-hydroxytryptamine while releasing a carbon dioxide and water. Finally, *P. cubensis* kinase (PsiK) converts 4-hydroxytryptamine into norbaeocystin using a phosphate donated by ATP.

use of a biosynthetic production route to continue studying the impact that psilocybin and structurally similar tryptamines have alone and in combination.

2. Results and discussion

2.1. Norbaeocystin production in E. coli

Prior to determining bioactivity of norbaeocystin in rats, we first developed a novel process for synthesizing pharmacologically relevant amounts of norbaeocystin, as existing synthetic methods were insufficient and resource intensive. Norbaeocystin production in *E. coli* was originally reported as a low-level accumulation of an undesired intermediate product in the psilocybin production pathway using the optimized psilocybin production strain, Psilo16 (Adams et al., 2019). After reconstructing a norbaeocystin-specific production strain, containing PsiD and PsiK and controlled by the consensus T7 promoter, low-level accumulation of norbaeocystin was observed (29.6 ± 5.2 mg/L) under standard fermentation conditions (Fig. 2b).

This resulted in a production strain and process that contains many similarities to the previously reported psilocybin production strain, including the same background host strain, plasmid background, base media composition, upstream untranslated region sequence, and many of the same co-factor and precursor requirements. Given these broad similarities between the previously reported psilocybin production process and the newly developed norbaeocystin production process, it was expected that a similar transcriptional optimization solution (i.e., similar promoter strength) would be found to be optimal.

To test this hypothesis, a transcriptional library comprised of five isopropyl ß-D-1-thiogalactopyranoside (IPTG)-inducible T7-*lac* promoter mutants of varied strength were used to construct two independent pooled libraries capable of norbaeocystin production: pETM6-xx^5-psiDK (operon configuration, 5 possible variants) and pETM6-xx^5-psiD-xx^5-psiK (pseudooperon configuration, 25 possible variants). These library promoters included the previously characterized (Jones et al., 2015) T7 mutant promoters G6, H9, H10, and C4, along with the Consensus (T7) sequence. Nearly 50 operon library colonies and 150 pseudooperon library colonies were screened, and their norbaeocystin production was quantified (Fig. 2a).

Similar to the development of a psilocybin overproducing strain, the norbaeocystin producing libraries showed a preference for the operon promoter configuration (Fig. 2a - red bars), resulting in the highest production strains with the lowest build-up of intermediate products when compared to their respective pseudo-operon libraries (Fig. 2a - gray bars). The sequencing results of top performing norbaeocystin production strains revealed an interesting trend with the top producing strain containing the strongest mutant promoter, C4, controlling the transcription of both *psiD* and *psiK* in operon configuration (Fig. 2b). Upon final rescreening, the top norbaeocystin producer, Nor1, showed a 7-fold improvement in norbaeocystin production over the original T7 consensus construct (Fig. 2b).

To further explore the transcriptional optimization landscape of the norbaeocystin and psilocybin producing strains, we constructed five psilocybin and five norbaeocystin pathways in operon configuration, each controlled by a different T7 mutant promoter (Fig. 2b). The data shows a mixed association between promoter strength and pathway performance, with two of the reduced strength promoters (G6, H10), as well as the strong T7 consensus promoter, leading to low levels of norbaeocystin production (Fig. 2b). As stated above, the strong C4 mutant promoter resulted in the highest norbaeocystin production levels. This is in contrast with the similarly constructed psilocybin pathway promoter library, which resulted in the best performance from the medium strength, H10, mutant promoter (Fig. 2b).

These results show little association between the two similar production pathways, indicating that there is much still to be learned surrounding the metabolic mechanisms of pathway optimization and balancing. Moreover, previously-reported studies for the production of another tryptophan-derived compound, violacein, found weakened promoters (G6 and H10) to result in significantly enhanced production over strong promoters when using an identical *E. coli* strain background

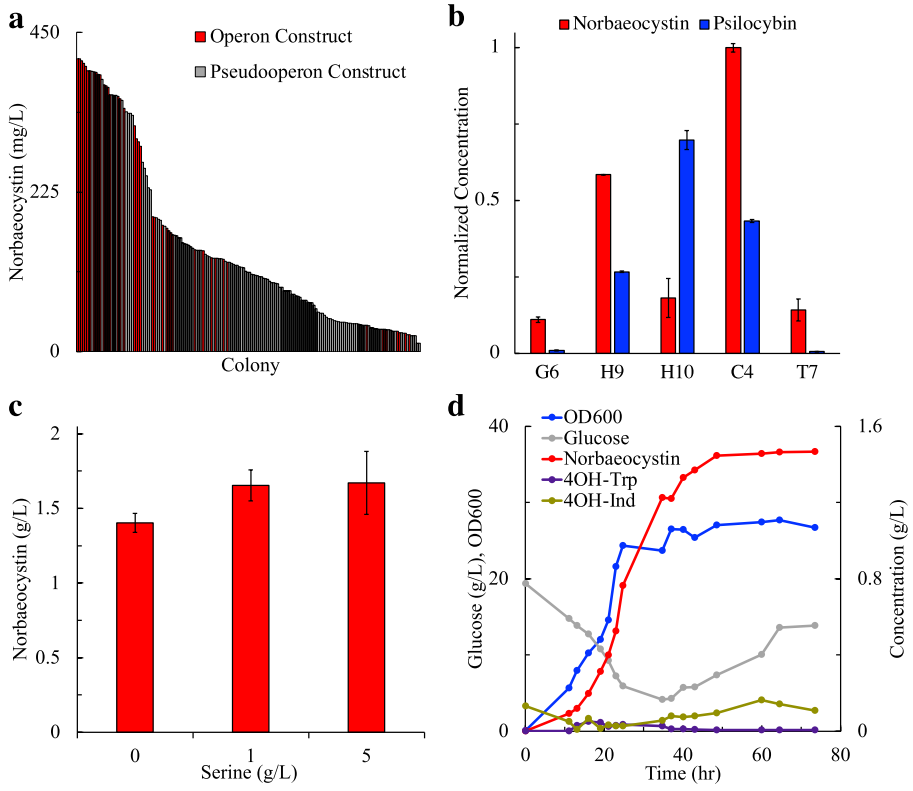

Fig. 2. Summary of genetic optimization and scale-up results. (a) Promoter library screening. Individual colonies from the operon (red bars) and pseudooperon (gray bars) libraries were selected and evaluated to discover elite production strains. Data for samples producing 0 mg/L of norbaeocystin (11.5% of total colonies screened) are not shown. (b) Normalized production of operon library members for norbaeocystin and psilocybin pathways organized in order of increasing promoter strength: G6 (low) – T7 (high). Constructs for each operon promoter configuration were identified and screened providing evidence that the transcriptional optimization solution for the norbaeocystin pathway differed from that of the psilocybin pathway. (c) Effect of varying supplemental serine concentration in the initial fermentation media on strain performance in the bioreactor. (d) Metabolite and growth curve profiles for a representative norbaeocystin bioreactor fed-batch fermentation. Data shown for one replicate of the 0 g/L serine condition. (For interpretation of the references to color in this figure legend, the reader is referred to the Web version of this article.)

and base plasmid (Jones et al., 2015). These conclusions motivate the random screening of a variety of promoter strengths and transcriptional unit configurations as a way to modulate or maximize pathway performance based on desired need. This re-optimization process is likely necessary regardless of the similarity to previously optimized strains.

2.2. Fermentation optimization studies

After selection and identification of Nor1 was complete, variations in media composition were tested in a shake flask study to maximize norbaeocystin production (Supplementary Fig. S2). This study included Andrew's Magic Media (AMM) as the control, AMM without the MOPS mix (AMM-no mix), and AMM without the MOPS/Tricine buffer component (AMM-no MOPS). Between these three media, a significant (p-value < 0.05) improvement was observed in the AMM-no MOPS condition, indicating that the buffering capacity of the MOPS/Tricine media component was unnecessary even under batch conditions (Supplementary Fig. S2). This is an interesting observation with positive impacts on scale up and cost competitiveness of the fermentation-based production process presented. The results from the media study were used to inform the selection of AMM-no MOPS for 1.5 L bioreactor studies using Nor1. These scaled up studies incorporated automated control of pH, foam, dissolved oxygen, and temperature, mimicking industrial conditions, while also enhancing cell growth and norbaeocystin production using a fed-batch process for glucose, ammonium phosphate dibasic, and the substrate 4-hydroxyindole.

In an attempt to further maximize norbaeocystin production in the bioreactor, the amino acid serine was identified as a necessary and potentially limiting substrate. Serine is one of the major substrates for the norbaeocystin biosynthesis pathway, condensing with 4-hydroxyindole to form 4-hydroxytryptophan through the promiscuous activity of the native tryptophan synthase (Fig. 1b). Additionally, serine plays an important role in metabolism as it is directly utilized for protein synthesis as it serves as the precursor molecule for several other amino acids including tryptophan, cystine, and glycine.

Due to the high demands on serine for both native metabolism and norbaeocystin biosynthesis, it was unclear if wild-type metabolism could support the necessary serine biosynthesis demand. To this end, various levels of serine were supplemented in the media and investigated at scale as a means to further evaluate this potential pathway bottleneck. Interestingly, no statistically significant difference ($p > 0.17$) was observed between differing serine supplementation levels, with an average of over 1.58 ± 0.08 g/L of norbaeocystin being produced across all serine supplementation conditions (Fig. 2c). Furthermore, 4-hydroxytryptophan, the pathway intermediate resulting from the promiscuous activity of tryptophan synthase (TrpB), was observed to build up throughout the fermentation when 4-hydroxyindole was provided in excess (Supplementary Fig. S4 – S6). This indicates that the norbaeocystin pathway serves as a sufficient serine sink to trigger natural serine biosynthesis and the resulting native flux towards serine exceeds the needs of both metabolism and the optimized exogenous pathway.

Comparing the metabolite profiles under differing serine supplementation levels, fermentation with enhanced serine supplementation tended to consume the initial 4-hydroxyindole substrate more quickly, building up a temporary excess of the 4-hydroxytryptophan intermediate (Supplementary Fig. S4 – S6). A representative temporal metabolite profile for a fed batch bioreactor trial is shown (Fig. 2d). Across all 6 bioreactor trials, an average productivity of 19.3 ± 2.1 mg/L/hr over the course of the fermentation run at a final substrate yield of $57.9 \pm 1.8\%$ mol norbaeocystin/mol 4-hydroxyindole was observed. These results represent the highest reported production metrics to date for norbaeocystin from any recombinant organism.

2.3. Rodent behavioral studies

Having developed a novel method to produce gram-scale quantities of both norbaeocystin and psilocybin (Adams et al., 2019), we set out to test the individual effectiveness of psilocybin and norbaeocystin at eliciting head twitch responses (HTRs) in rats. HTRs were assessed for 60 min, beginning immediately following oral administration of each substance. In the first set of studies, drug was delivered via gavage in an undiluted filtered broth media (volume varied by dosage). This vehicle was used to determine if gavage of broth was safe and effective, as it would reduce the downstream processing required for initial compound screening. When delivered in a broth vehicle, psilocybin elicited dose-dependent effects on HTRs [1-way ANOVA, $F\ (4,24) = 5.18$, $p = 0.0037$, Fig. 3a]. Post hoc tests showed that 1.0 mg/kg psilocybin increased HTRs compared to 0 mg/kg (vehicle alone, $p = 0.0003$), 0.1 mg/kg ($p = 0.008$), 0.2 mg/kg ($p = 0.034$), and 2.0 mg/kg ($p = 0.002$). This pattern of effects was not observed after norbaeocystin administration (Fig. 3b), which failed to increase the rate of HTRs at any dose studied [$F\ (4,26) = 1.861$, $p = 0.1475$]. In addition to HTRs, locomotor behavior was also assessed with results showing no significant effect of either psilocybin or norbaeocystin (Supplemental Fig. S8).

It is important to note that the broth vehicle used in the above study may have confounded our results due to inadvertent inclusion of other active compounds, including low levels of baeocystin in the psilocybin broth. Additionally, since the concentration of the drugs were constant across dosages, this meant that the volume administered to each animal varied by dose, which could cause differential absorption and behavioral effects. Therefore, in a second set of studies, drug was purified from the media, and delivered via gavage in a distilled water vehicle. In this study, the volume gavaged was held constant across dosages (1 mL/kg). In these studies, the same basic pattern of results was observed. Psilocybin caused dose-dependent increases in HTRs [1-way ANOVA $F\ (4,18) = 6.073$, $p = 0.0028$, Fig. 4a], with post hoc tests showing that compared to vehicle alone, psilocybin significantly increased HTRs at 0.2 mg/kg ($p = 0.044$), 1 mg/kg ($p = 0.0007$), and 2 mg/kg ($p = 0.002$). Additionally, both 1 mg/kg and 2 mg/kg increased HTRs compared to 0.1 mg/kg ($p = 0.0047$ and $p = 0.014$, respectively). Norbaeocystin did not increase the occurrence of HTRs at any dose studied [$F\ (4,14) = 0.2385$, $p = 0.91$, Fig. 4b). Lastly, we compared the dose-response curves of psilocybin across studies (2-way ANOVA), and found no significant effect of vehicle [$F\ (1,42) = 2.499$, $p = 0.12$], or interaction between dosage and vehicle [$F\ (4,42) = 1.89$, $p = 0.13$], suggesting that variation in the behavioral effects of the drug may have been driven by other variables (cohort, etc.).

This work presents dose-response curves for both psilocybin and norbaeocystin derived from an *E. coli* production system in unpurified (broth) and purified (water) forms. Our results demonstrate that *E. coli*-derived psilocybin dose-dependently affects HTRs, while norbaeocystin shows no dose-dependent effect. These results suggest that although psilocybin and norbaeocystin share many structural similarities, their interaction with the 5-HT2A system is different. They may, however, interact in other ways. For example, it is known that psilocybin is dephosphorylated to psilocin by alkaline phosphatase (Horita and Weber, 1961a, 1961b; Kolaczynska et al., 2021), which is further metabolized primarily by monoamine oxidase (Hasler et al., 1997; Kalberer et al., 1962) or glucuronosyltransferases (Manevski et al., 2010). Given their shared structure, it is highly likely that norbaeocystin shares a similar metabolic process; however, no prior studies have investigated this. Should such overlap exist, the presence of both compounds could impact the metabolism of each other through competitive interactions. This likely similarity in metabolic activation and detoxification, respectively, suggests there may be value to studying the effects of these drugs in combination.

A major outcome of our results is that they demonstrate the pharmacological efficacy of *E. coli*-derived psilocybin and norbaeocystin. Synthetically produced psilocybin is known to elicit responses similar to those presented here (Sherwood et al., 2020), but it is also expensive and time-consuming to produce. The *E. coli*-derived psilocybin used by this study can be rapidly produced in large amounts at concentrations that

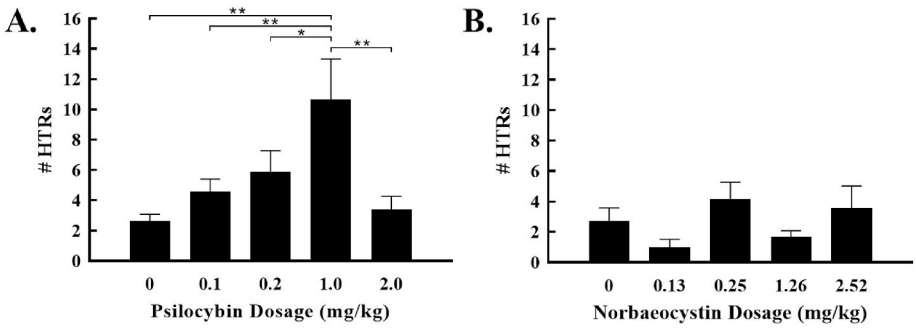

Fig. 3. Dose-dependent effects of tryptamines alone and in combination when administered in a broth vehicle. (a) Psilocybin caused significant increases in the number of head twitches at 1.0 mg/kg. (b) Norbaeocystin did not increase the number of head twitches at any dose studied. Note: *p < 0.05; **p < 0.01.

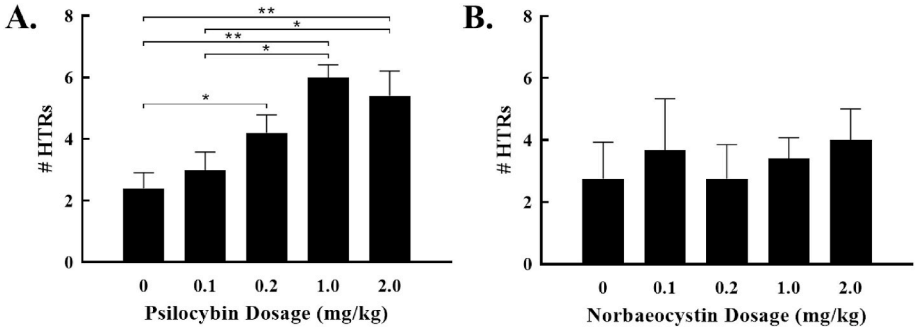

Fig. 4. Dose-dependent effects of tryptamines alone and in combination when administered in a water vehicle. (a) Psilocybin caused significant increases in the number of head twitches at 0.2, 1.0, and 2.0 mg/kg. (b) Norbaeocystin did not increase the number of head twitches at any dose studied. Note: *p < 0.05; **p < 0.01.

are pharmacologically relevant. By verifying the efficacy of *E. coli*-derived psilocybin, these results confirm that the method presented in this work is a viable means of producing psilocybin and norbaeocystin, and likely other pharmaceutically relevant molecules. Use of these production methods will improve access to psilocybin and other tryptamine compounds and lower barriers to their use in a variety of pre-clinical, clinical, and non-clinical settings.

Another significant outcome of our results is that they illustrate the relative safety of directly gavaging filtered *E. coli* broth as a drug vehicle. To our knowledge, the use of filtered cell culture media as a drug vehicle has never before been published. We observed no immediate or lasting effects after the gavage of any solution used in this study, including the negative control cell broth. No overt measure of rodent health was significantly affected, including body weight (Supplemental Fig. S9), stool consistency, and urinary output. Additionally, results obtained using purified psilocybin from our biosynthesis process demonstrated analogous trends to that from the broth-based samples. It is important to note that the use of complex vehicles, such as cell broth, does introduce added variables due to batch-to-batch variability of cellular and pathway metabolite concentrations, however it could serve as a rapid and economical initial screening vehicle for drug candidate compounds. As the use of recombinant microorganisms for chemical production becomes more common, the use of cell culture media as a drug vehicle for oral delivery could dramatically reduce the barrier to entry for initial screening of novel compounds in animal models by reducing time and costs associated with purification.

Despite the significance of our findings and their implications, our study is not without limitations. It is important to note that the psilocybin-containing broth used here contains trace amounts of norbaeocystin and baeocystin, such that the psilocybin alone group may have been unintentionally enhanced by small entourage effects. Additionally, our studies leveraged only male rats and may not translate to females or other species. Despite these limitations, our study suggests that future studies should investigate the potential therapeutic utility of psilocybin-related drug combinations. It is essential that other tryptamines present in the psilocybin biosynthesis pathway are investigated, to determine if they demonstrate interactions which impact the activity of psilocybin. While these results are interesting from a basic pharmacological perspective, they also have potential relevance to the clinical use of these drugs.

3. Conclusion

Now more than ever, society is impacted by the rising cases of depression and anxiety due, in part, to the ongoing COVID-19 pandemic (Chen et al., 2020; Fitzpatrick et al., 2020; Rossen et al., 2020; Rudenstine et al., 2020). Previous clinical studies using a psilocybin-only drug product have demonstrated promising outcomes for patients struggling with treatment-resistant depression and anxiety (Carhart-Harris et al., 2017). The results presented here can enable studies to show the combinatorial impacts between psilocybin, norbaeocystin, and other similar tryptamines. Such a strategy may carry benefits in other natural product-based therapeutic approaches as well, which often contain major and minor bioactive metabolites. Thus, the results provided here may have broad impacts on the field of medicinal pharmacology.

4. Methods

4.1. Bacterial strains, vectors, and media

All plasmids presented in this study were propagated with *E. coli* DH5α, while all chemical production experiments used *E. coli* BL21 Star™ (DE3) as the production host. Unless otherwise noted, Andrew's Magic Media (AMM) (He et al., 2015) was used for both overnight growth and production media, while Luria Broth (LB) was used for plasmid propagation during cloning. The antibiotic ampicillin (80 μg/mL) was used to select for all pET-based vectors. A description of all

plasmids and strains used in this study can be found in Table S1.

4.2. Plasmid and pooled library construction and screening

Plasmids containing the norbaeocystin production pathway were constructed using the previously reported pETM6-SDM2x plasmid backbone (Adams et al., 2019). Single gene constructs were assembled using traditional restriction ligation cloning using *Nde*I and *Xho*I. All multigene plasmids were constructed in either operon or psuedooperon configuration using a modified version of the previously published ePathBrick (isocaudomer-based) methods while all pooled promoter libraries were constructed using standard ePathOptimize methods (Jones et al., 2015; Xu et al., 2012) analogous to those used for the construction of the psilocybin production plasmid libraries as reported previously (Adams et al., 2019; Jones et al., 2015).

The plasmid DNA libraries were then transformed into the commercially available production host strain BL21 Star™ (DE3) and screened in a 48-well plate fermentation assay using standard media conditions as reported below. Upon identification of the top seven mutants from the promoter library, the strains were rescreened to confirm high production levels prior to plasmid isolation and transformation into *E. coli* DH5α for permanent storage. The plasmid DNA was then isolated from the DH5α strain for promoter sequencing and retransformed into BL21 Star™ (DE3) for a final round of screening.

4.3. Standard screening conditions

Standard screening was performed using 48-well plates with a rectangular cross section and a 2 mL working volume at 37 °C. Serine (1 g/L), 4-hydroxyindole (350 mg/L), and ampicillin (80 μg/mL) were supplemented in AMM-No MOPS for all experiments, unless otherwise noted. Overnight cultures were grown for 12–16 h at 37 °C in a shaker incubator (225 rpm) in the same media that was used for final production. Induction with 1 mM IPTG occurred 4 h after inoculation. Samples were taken at 24 and 48 h, unless otherwise noted, and subjected to HPLC and LC-MS analysis.

4.4. Scale-up studies

All bioreactor studies were performed in an Eppendorf BioFlo120 bioreactor with 1.5 L working volume. The vessel was mixed using a direct drive shaft containing two Rushton-type impellers positioned equidistance under the liquid surface. The overnight cultures were grown for 9–12 h in a 250 mL baffled shake flask at 37 °C in a modified AMM supplemented with serine (0–5 g/L), thiamine (15 mg/L), and ampicillin (80 μg/mL), as noted. The bioreactor was then inoculated at 2% v/v to an initial OD_{600} of approximately 0.05–0.10 and induced 4 h post-inoculation using 1 mM IPTG. Temperature, pH, and dissolved oxygen (DO) were held constant at 37 °C, 6.5, and 30%, respectively. pH, DO, and foam were maintained automatically by the addition of 10 M NaOH, an agitation cascade (300–1000 rpm), and addition of Antifoam 204. Full oxygen saturation was defined under the conditions of 37 °C, 300 rpm agitation, pH 7.0, and 2 v/v per minute of standard air. The zero-oxygen set point was calibrated using a nitrogen gas flush. Samples were collected periodically for measurement of OD_{600} and metabolite concentrations. Once the initial 20 g/L of glucose was exhausted, as determined by HPLC, a separate feed stream of 500 g/L glucose and 90 g/L $(NH_4)_2HPO_4$ was set to a flow rate ranging from 2.0 to 4.0 mL/L/hr. Once the initial 150 mg/L of 4-hydroxyindole was consumed and build-up of the key intermediate, 4-hydroxytryptophan, was low (approx. 12 h), 4-hydroxyindole (40 mg/mL in EtOH) was periodically adjusted from 0 up to 47 mg/L/hr using an external syringe pump. The concentration of norbaeocystin, all pathway intermediates, and glucose were quickly analyzed via HPLC after each sample was taken with an approximate 45-min delay. This allowed for modifications to be made to the reaction vessel in near real-time to feed rates for glucose and 4-hydroxyindole.

4.5. Analytical methods

Metabolite analysis was performed on a Thermo Scientific Ultimate 3000 High-Performance Liquid Chromatography (HPLC) system equipped with Diode Array Detector (DAD), Refractive Index Detector (RID), and Thermo Scientific ISQ™ EC single quadrupole mass spectrometer (MS). Samples were prepared for HPLC and LC-MS analysis by using a 3:1 ratio of MilliQ water to sample broth, vortexed briefly, and then centrifuged at 15,000×*g* for 5 min. A volume of 2 μL of the resulting supernatant was then injected for HPLC and LC-MS analysis. Authentic Standards were purchased for psilocybin (Cerilliant). Norbaeocystin was quantified using a standard purified and characterized as described below.

Quantification of aromatic metabolites was performed using absorbance at 280 nm from the DAD and the metabolites were separated using an Agilent Zorbax Eclipse XDB-C18 analytical column (3.0 mm × 250 mm, 5 μm) with mobile phases of water (A) and acetonitrile (B) both containing 0.1% formic acid at a rate of 1 mL/min: 0 min, 5% B; 0.43 min, 5% B; 5.15 min, 19% B; 6.44 min, 100% B; 7.73 min, 100% B; 7.73 min, 5% B; 9.87 min, 5% B. This method resulted in the following observed retention times as verified by analytical standards (when commercially available) and MS analysis (as described below): 4-hydroxyindole (6.6 min), 4-hydroxytryptophan (3.4 min), 4-hydroxytryptamine (3.2 min), norbaeocystin (1.6 min), baeocystin (1.9 min) and psilocybin (2.2 min).

Liquid Chromatography Mass Spectrometry (LC-MS) data was collected where the full MS scan was used to provide an extracted ion chromatogram (EIC) of our compounds of interest. Analytes were measured in positive ion mode at the flow rate, solvent gradient, and column conditions described above. The instrument was equipped with a heated electrospray ionization (HESI) source and supplied ≥99% purity nitrogen from a Peak Scientific Genius XE 35 laboratory nitrogen generator. The source and detector conditions were as follows: sheath gas pressure of 80.0 psig, auxiliary gas pressure of 9.7 psig, sweep gas pressure of 0.5 psig, foreline vacuum pump pressure of 1.55 Torr, vaporizer temperature of 500 °C, ion transfer tube temperature of 300 °C, source voltage of 3049 V, and source current of 15.90 μA.

A Bio-Rad Aminex HPX-87H column coupled with a RI detector was used for quantification of sugars and organic acids as described in previous work (Adams et al., 2019). All error is reported as the group mean ± standard error of the mean.

4.6. Norbaeocystin purification

Approximately 1.6 g/L norbaeocystin in 500 mL of *E. coli* broth was centrifuged (5,000×*g*, 30 min), and filtered through a 0.2 μm bottle top filter to remove cells and extracellular particulates. The broth was then dried under a vacuum in a round bottom flask. The dried broth was continually mixed with 160 mL of hot (50 °C) ethanol for 30 min. The mixture was then filtered through grade 615 filter paper in a Buchner funnel. The filtrate was collected and analyzed by HPLC to confirm a lack of norbaeocystin. The filter cake was then collected and resuspended in 50 mL of water, resulting in some insoluble product that was discarded. The resuspension was quantified by HPLC, as described above, and a concentration of approximately 11.5 g/L was found, resulting in a ~70% yield.

This norbaeocystin concentrate was then purified by preparative HPLC using an Agilent Polaris C18-A column (250 mm × 21.2 mm, 5 μm) with mobile phases of water (A) and acetonitrile (B), both containing 0.1% formic acid at a flow rate of 10 mL/min: 0 min, 5% B; 0.9 min, 5% B; 10 min, 40% B; 11.25 min, 100% B; 14.5 min, 100% B; 14.5 min, 5% B; 17 min, 5% B. Injections of 500 μL were used, resulting in a retention time of approximately 9.2 min for norbaeocystin. The fraction collection was triggered by peak height in the UV absorbance spectrum

at 280 nm. The collected fractions were then pooled and dried under vacuum prior to analysis by LC-MS, ^{1}H NMR (Supplementary Fig. S13), and ^{13}C NMR (Supplementary Fig. S14). The sample accounted for ~94% of the ^{1}H NMR peak area and ~98% of the HPLC A280 peak area observed in the respective spectrums. ^{1}H NMR (400 MHz, D_2O) δ (ppm) 7.18 (1H, d, $J = 8.2$ Hz), 7.13 (1H, s), 7.08 (1H, m), 6.94 (1H, d, $J = 8.2$ Hz), 3.26 (2H, t, $J = 7.2$ Hz), 3.18 (2H, t, $J = 7.1$ Hz); ^{13}C NMR (125 MHz, D_2O) δ (ppm) 145.74, 138.65, 124.25, 122.51, 118.55, 108.86, 108.63, 107.84, 40.85, 23.89; LC-MS (ESI) calculated for $C_{10}H_{14}N_2O_4P^+$ 257.069 $[M + H]^+$, found 257.1.

4.7. Psilocybin purification

Approximately 0.9 g/L psilocybin in 1000 mL of *E. coli* broth was centrifuged (5,000×*g*, 30 min), and filtered through a 0.2 μm bottle top filter to remove cells and extracellular particulates. The broth was then dried under a vacuum in a round bottom flask. The dried broth was continually mixed with 450 mL of methanol for 30 min, resulting in a granular insoluble fraction and a colored liquid fraction. The mixture was then filtered through grade 615 filter paper in a Buchner funnel. The filtrate was collected and dried under reduced pressure resulting in an oily solid (~60% yield). The solid was then resuspended in approximately 45 mL of water and filtered to remove any insoluble particulates prior to preparative HPLC purification as described above for norbaeocystin.

The collected fractions were then pooled and concentrated under vacuum until spontaneous crystallization. The white crystals were filtered from solution, rinsed with water, and freeze dried prior to analysis by LC-MS and ^{1}H NMR (Supplementary Fig. S16). The sample accounted for ~98.8% of the ^{1}H NMR peak area and ~99+% of the HPLC A280 peak area observed in the respective spectrums. ^{1}H NMR (500 MHz, D_2O) δ (ppm) 7.19 (1H, d, $J = 8.1$ Hz), 7.14 (1H, s), 7.09 (1H, t, $J = 8.0$ Hz), 6.94 (1H, d, $J = 7.8$ Hz), 3.40 (2H, t, $J = 7.5$ Hz), 3.24 (2H, t, $J = 7.5$ Hz), 2.82 (6H, s); LC-MS (ESI) calculated for $C_{12}H_{18}N_2O_4P^+$ 285.1004 $[M + H]^+$, found 285.0996.

4.8. E. coli broth preparation for HTR studies

For use in the animal studies, control, psilocybin-containing, and norbaeocystin-containing broths were produced from fed batch bioreactor fermentations of Psilo16 (no 4-hydroxyindole supplement), Psilo16 (4-hydroxyindole supplement), and Nor1 (4-hydroxyindole supplement), respectively, using the conditions specified previously for psilocybin (Adams et al., 2019) and here for norbaeocystin. After the fermentation was concluded, the broth was centrifuged (5000×*g*, 30 min) and filtered using a 0.2 μm bottle top filter, prior to administration to animals (described below). Filtered broth samples were stored at room temperature up to two months between production and use with negligible degradation observed. Metabolite concentrations in the broth were periodically quantified using HPLC analysis.

Representative HPLC chromatograms for the negative control, norbaeocystin, and psilocybin containing broth are shown in Supplementary Fig. S15. The psilocybin containing broths also contained trace levels of norbaeocystin (<20 mg/L) and aeruginascin (<1 mg/L), low levels of baeocystin (approx. 150 mg/L), and high levels of psilocybin (approx. 1 g/L). The norbaeocystin containing broths had high levels of norbaeocystin (approx. 1.5 g/L) with no baeocystin, psilocybin, or aeruginascin due to the lack of the methyltransferase responsible for the synthesis of the latter metabolites. The control broth contained none of the aforementioned metabolites.

4.9. Rodent behavioral studies

4.9.1. Subjects

A total of 22 adult (PND 90–120) male Long Evans rats (Charles River Laboratories, Raleigh, NC) were used in these experiments. All animals were individually housed in standard rat cages throughout testing to protect cranial implants and kept on a 12 h:12 h light/dark cycle. Food and water were available *ad libitum* throughout all experiments. Animals were divided into 4 treatment groups: psilocybin in broth (n = 6), norbaeocystin in broth (n = 6), psilocybin in water (n = 5), and norbaeocystin in water (n = 5). All procedures and protocols were conducted in accordance with the National Institutes of Health's Guidelines for the Care and Use of Laboratory Animals and the Animal Welfare Act and were approved by Miami University's Institutional Animal Care and Use Committee.

4.9.2. Surgery

Prior to beginning surgery, animals were given 48 h access to acetaminophen via drinking water (37 mg/mL, Children's Dye Free Pain and Fever Reliever, Walgreen Co.) for preventive pain relief. All surgeries were then conducted on isoflurane anesthetized animals (5% for induction and 3% for maintenance). Once deeply sedated, animals were secured in a stereotaxic frame and the surgical site sterilized. The skull was then exposed, and four holes were drilled into the periphery of the skull in a rectangular formation and 4 stainless steel screws (1/8" 1–72) were inserted into each of the holes. A single neodymium magnet (MGLN10-5-5, MiSUMi Corp.) was then placed on top of the screws. Both the screws and the magnet were then covered in dental acrylic to secure them to the skull. Once complete, animals were returned to their home cage and closely monitored for the following 3 days. During this period, they were provided acetaminophen (37 mg/mL), as described above. Animals were given a one-week recovery following surgery before beginning behavioral testing.

4.9.3. Drugs and drug administration

Animals receiving drug in a filtered *E. coli* broth vehicle received either vehicle alone (control broth at 1 mL/kg) or doses of their associated drug condition as follows: 0.1, 0.2, 1, 2 mg/kg psilocybin; 0.13, 0.25, 1.26, 2.52 mg/kg norbaeocystin. Animals received no more than 3 treatments, and the order of drug presentation was randomized across subjects, with one week separating each drug exposure to prevent the development of tolerance or sensitization (Gewirtz and Marek, 2000). Total volume of each gavage ranged from 0.1 to 2.0 mL/kg, depending on dosage and animal body weight.

Animals receiving drug in distilled water received either vehicle alone or 0.1, 0.2, 1, 2 mg/kg psilocybin; 0.1, 0.2, 1, 2 mg/kg psilocybin. As above, animals received no more than 5 treatments, and the order of drug presentation was randomized across subjects, with one week separating each drug exposure. Gavage volume across all dosages was 1.0 mL/kg.

4.9.4. Head twitch response testing

Head movements were recorded using a magnetometer-based approach described previously (Halberstadt and Geyer, 2013). This magnetometer-based approach is considerably more sensitive and easier to quantify than hand-coding high-speed video recordings (Halberstadt and Geyer, 2013). After surgical implantation of a skull-mounted magnet and recovery (see above), rats were administered drug or vehicle and placed in a large polycarbonate tube (~56 cm diameter, ~30 cm height) surrounded by ~2000 turns of #30 enameled magnet wire (Supplementary Fig. S11 – S12). Changes in the position of the animal caused changes in the voltage across the wire, which was minimally amplified with a gain of 2, bandpass filtered with a cutoff frequency of 10 kHz to exclude noise (as previously described (Halberstadt and Geyer, 2013)), recorded at 1000 S/s, and analyzed as detailed below. HTRs were observed for 60 min, beginning immediately after drug delivery.

4.9.5. Locomotor testing

At least one week following HTR testing, animals conducted a one-day locomotor test in 14″ × 14″ x 8" locomotion chambers (Accuscan, Omnitech Electronics, Inc, Columbus, OH). Animals were allowed to

habituate to the apparatus for 15 min. They were then removed from the locomotion chambers, administered drug as described above, and placed immediately back into the chamber for 60 min.

4.9.6. Data analysis

Continuous recordings of HTRs (voltage) were exported to Offline Sorter (v4.5, Plexon Inc, Dallas, TX) for determination of the time of each HTR based on waveform characteristics. Specifically, head twitches were identified from voltage recordings by a single observer, blinded to subject condition, by the presence of 1) amplitude exceeds background noise; 2) fundamental frequency of 20–40 Hz; 3) more than 2 bipolar peaks; and 4) duration <120 ms. The total number of HTRs was compared across doses within each drug condition using analysis of variance (Graphpad Prism 8), followed by post hoc tests when appropriate, corrected for multiple comparisons using the FDR method (Benjamini and Hochberg, 1995). Body weight was analyzed independently for each drug condition using 2-way repeated measures mixed models, including factors for group and time since gavage (days). Locomotor data were analyzed using 1-way ANOVA, including analyses for the total distance travelled and the number of rearing events during the post-drug administration period (there was no difference between groups during the habituation period). Group means ± standard error of the mean are presented in all figures.

CRediT author statement

Alexandra M. Adams: Data curation, Formal analysis, Investigation, Writing - original draft, Writing - review & editing. **Nicholas A. Anas:** Data curation, Formal analysis, Investigation, Writing - original draft, Writing - review & editing. **Abhishek K. Sen:** Data curation, Investigation, Writing - review & editing. **Jordan D. Hinegardner-Hendricks:** Data curation, Formal analysis, Investigation, Writing - review & editing. **Philip J. O'Dell:** Investigation, Writing - review & editing. **William J. Gibbons Jr.:** Investigation, Resources, Writing - review & editing. **Jessica E. Flower:** Investigation, Writing - review & editing. **Matthew S. McMurray:** Conceptualization, Formal analysis, Funding acquisition, Investigation, Project administration, Supervision, Writing - original draft, Writing - review & editing. **J. Andrew Jones:** Conceptualization, Formal analysis, Funding acquisition, Investigation, Project administration, Supervision, Writing - original draft, Writing - review & editing.

Declaration of competing interest

JAJ is the chairman of the scientific advisory board and a significant stakeholder at PsyBio Therapeutics. MSM is a member of the scientific advisory board at PsyBio Therapeutics. PsyBio Therapeutics has licensed psilocybin biosynthesis-related technology from Miami University. JAJ, MSM, AMA, PJO, WJGJ, and JEF are co-inventors on several related patent applications. All other authors declare no conflicts of interest.

Acknowledgments

This work was supported by Miami University start-up funds from the Department of Chemical, Paper, and Biomedical Engineering (JAJ), Undergraduate Summer Support from the College of Engineering and Computing (AMA, PJO), and a sponsored research grant from PsyBio Therapeutics (JAJ, MSM). Requests for strains and plasmids capable of producing controlled substances (e.g., psilocybin, norbaeocystin) will require proof of appropriate approvals and licenses from all necessary state and federal agencies prior to completion of a materials transfer agreement. The authors would also like to thank Dr. Kathryn E. Jones for helpful comments and discussions on the final draft, Dr. Anne M. Carroll for NMR spectroscopy and analysis, Dr. Adam L. Halberstadt for advice and guidance on automated HTR measurements and data analysis, the Miami University Instrumentation Lab staff (Michael Weeks, Jayson Alexander, and Kyle Turner) for construction and troubleshooting of the HTR magnetometer, and Piper Hamilton, Kellar McCloy, Jessica Crowder, and Sarah Loberger for their assistance with the rodent data collection.

Appendix A. Supplementary data

Supplementary data to this article can be found online at https://doi.org/10.1016/j.mec.2022.e00196.

References

Adams, A.M., Kaplan, N.A., Wei, Z., Brinton, J.D., Monnier, C.S., Enacopol, A.L., Ramelot, T.A., Jones, J.A., 2019. In vivo production of psilocybin in E. coli. Metab. Eng. 56, 111–119. https://doi.org/10.1016/j.ymben.2019.09.009.

Benjamini, Y., Hochberg, Y., 1995. Controlling the false discovery rate: a practical and powerful approach to multiple testing. J. R. Stat. Soc. Ser. B 57, 289–300. https://doi.org/10.1111/j.2517-6161.1995.tb02031.x.

Canal, C.E., Morgan, D., 2012. Head-twitch response in rodents induced by the hallucinogen 2,5-dimethoxy-4-iodoamphetamine: a comprehensive history, a re-evaluation of mechanisms, and its utility as a model. Drug Test. Anal. https://doi.org/10.1002/dta.1333.

Carhart-Harris, R.L., Roseman, L., Bolstridge, M., Demetriou, L., Pannekoek, J.N., Wall, M.B., Tanner, M., Kaelen, M., McGonigle, J., Murphy, K., Leech, R., Curran, H. V., Nutt, D.J., 2017. Psilocybin for treatment-resistant depression: fMRI-measured brain mechanisms. Sci. Rep. 7, 13187. https://doi.org/10.1038/s41598-017-13282-7.

Chen, Y., Zhou, H., Zhou, Y., Zhou, F., 2020. Prevalence of self-reported depression and anxiety among pediatric medical staff members during the COVID-19 outbreak in Guiyang, China. Psychiatr. Res. https://doi.org/10.1016/j.psychres.2020.113005.

de la Fuente Revenga, M., Shin, J.M., Vohra, H.Z., Hideshima, K.S., Schneck, M., Poklis, J.L., González-Maeso, J., 2019. Fully automated head-twitch detection system for the study of 5-HT2A receptor pharmacology in vivo. Sci. Rep. 9, 1–14. https://doi.org/10.1038/s41598-019-49913-4.

Fitzpatrick, K.M., Drawve, G., Harris, C., 2020. Facing new fears during the COVID-19 pandemic: the State of America's mental health. J. Anxiety Disord. 75, 102291. https://doi.org/10.1016/j.janxdis.2020.102291.

Gartz, J., 1994. Extraction and analysis of indole derivatives from fungal biomass. J. Basic Microbiol. 34, 17–22. https://doi.org/10.1002/jobm.3620340104.

Gewirtz, J.C., Marek, G.J., 2000. Behavioral evidence for interactions between a hallucinogenic drug and group II metabotropic glutamate receptors. Neuropsychopharmacology 23, 569–576. https://doi.org/10.1016/S0893-133X(00)00136-6.

González-Maeso, J., Weisstaub, N.V., Zhou, M., Chan, P., Ivic, L., Ang, R., Lira, A., Bradley-Moore, M., Ge, Y., Zhou, Q., Sealfon, S.C., Gingrich, J.A., 2007. Hallucinogens recruit specific cortical 5-HT2A receptor-mediated signaling pathways to affect behavior. Neuron 53, 439–452. https://doi.org/10.1016/j.neuron.2007.01.008.

Halberstadt, A.L., Geyer, M.A., 2011. Multiple receptors contribute to the behavioral effects of indoleamine hallucinogens. Neuropharmacology 61, 364–381. https://doi.org/10.1016/j.neuropharm.2011.01.017.

Halberstadt, A.L., Geyer, M.A., 2013. Characterization of the head-twitch response induced by hallucinogens in mice: detection of the behavior based on the dynamics of head movement. Psychopharmacology (Berl) 227, 727–739. https://doi.org/10.1007/s00213-013-3006-z.

Hasler, F., Bourquin, D., Brenneisen, R., Bär, T., Vollenweider, F.X., 1997. Determination of psilocin and 4-hydroxyindole-3-acetic acid in plasma by HPLC-ECD and pharmacokinetic profiles of oral and intravenous psilocybin in man. Pharm. Acta Helv. 72, 175–184. https://doi.org/10.1016/S0031-6865(97)00014-9.

He, W., Fu, L., Li, G., Andrew Jones, J., Linhardt, R.J., Koffas, M., 2015. Production of chondroitin in metabolically engineered E. coli. Metab. Eng. 27, 92–100. https://doi.org/10.1016/j.ymben.2014.11.003.

Horita, A., Weber, L.J., 1961a. Dephosphorylation of psilocybin to psilocin by alkaline phosphatase. Proc. Soc. Exp. Biol. Med. 106, 32–34. https://doi.org/10.3181/00379727-106-26228.

Horita, A., Weber, L.J., 1961b. The enzymic dephosphorylation and oxidation of psilocybin and pscilocin by mammalian tissue homogenates. Biochem. Pharmacol. 7, 47–54. https://doi.org/10.1016/0006-2952(61)90124-1.

Jones, J.A., Vernacchio, V.R., Lachance, D.M., Lebovich, M., Fu, L., Shirke, A.N., Schultz, V.L., Cress, B., Linhardt, R.J., Koffas, M.A.G., 2015. ePathOptimize: a combinatorial approach for transcriptional balancing of metabolic pathways. Sci. Rep. 5, 11301. https://doi.org/10.1038/srep11301.

Kalberer, F., Kreis, W., Rutschmann, J., 1962. The fate of psilocin in the rat. Biochem. Pharmacol. 11, 261–269. https://doi.org/10.1016/0006-2952(62)90050-3.

Kolaczynska, K.E., Liechti, M.E., Duthaler, U., 2021. Development and validation of an LC-MS/MS method for the bioanalysis of psilocybin's main metabolites, psilocin and 4-hydroxyindole-3-acetic acid, in human plasma. J. Chromatogr. B 1164, 122486. https://doi.org/10.1016/J.JCHROMB.2020.122486.

Leung, A.Y., Paul, A.G., 1968. Baeocsytin and norbaeocystin: new analogs of psilocybin from. Psilocybe baeocystis 57, 1667–1671.

Manevski, N., Kurkela, M., Höglund, C., Mauriala, T., Court, M.H., Yli-Kauhaluoma, J., Finel, M., 2010. Glucuronidation of psilocin and 4-hydroxyindole by the human UDP-glucuronosyltransferases. Drug Metab. Dispos. 38, 386–395. https://doi.org/10.1124/dmd.109.031138.

Milne, N., Thomsen, P., Mølgaard Knudsen, N., Rubaszka, P., Kristensen, M., Borodina, I., 2020. Metabolic engineering of Saccharomyces cerevisiae for the de novo production of psilocybin and related tryptamine derivatives. Metab. Eng. 60, 25–36. https://doi.org/10.1016/j.ymben.2019.12.007.

Rossen, J.W.A., Tedim, A.P., Murray, A.K., 2020. The novel coronavirus COVID-19 outbreak: global implications for antimicrobial resistance. Front. Microbiol 1020. https://doi.org/10.3389/fmicb.2020.01020. www.frontiersin.org.

Rudenstine, S., McNeal, K., Schulder, T., Ettman, C.K., Hernandez, M., Gvozdieva, K., Galea, S., 2020. Depression and anxiety during the COVID-19 pandemic in an urban, low-income public university sample. J. Trauma Stress 22600. https://doi.org/10.1002/jts.22600, 2020, jts.

Sherwood, A.M., Halberstadt, A.L., Klein, A.K., McCorvy, J.D., Kaylo, K.W., Kargbo, R.B., Meisenheimer, P., 2020. Synthesis and biological evaluation of tryptamines found in hallucinogenic mushrooms: norbaeocystin, baeocystin, norpsilocin, and aeruginascin. J. Nat. Prod. acs.jnatprod., 9b01061 https://doi.org/10.1021/acs.jnatprod.9b01061.

Wurst, M., Kysilka, R., Flieger, M., 2002. Psychoactive tryptamines from basidiomycetes. Folia Microbiol. https://doi.org/10.1007/BF02818560.

Xu, P., Vansiri, A., Bhan, N., Koffas, M.A.G., 2012. ePathBrick: a synthetic biology platform for engineering metabolic pathways in E. coli. Biol 1, 256–266. https://doi.org/10.1021/sb300016b.